Available online at www.sciencedirect.com
ScienceDirect
Surface Science 601 (2007) 3261–3267
SURFACE SCIENCE
www.elsevier.com/locate/susc

Characterization of Au nano-cluster formation on and diffusion in polystyrene using XPS peak shape analysis

Shaaker Hajati [a,b,*], Vladimir Zaporojtchenko [c], Franz Faupel [c], Sven Tougaard [a]

[a] Department of Physics and Chemistry, University of Southern Denmark, DK-5230 Odense M, Denmark
[b] Department of Physics, Yasouj University, Yasouj, Iran
[c] Lehrstuhl für Materialverbunde, Technische Fakultät der CAU, Kaiserstr 2, D-24143 Kiel, Germany

Received 11 May 2007; accepted for publication 1 June 2007
Available online 7 June 2007

Abstract

XPS peak shape analysis is used as a novel and nondestructive method to study Au nano-cluster growth mechanism on polystyrene (PS) as a function of deposition as well as diffusion and distribution of the nano-clusters in PS as a function of subsequent annealing at temperatures in the range from room temperature to above the glass transition temperature of PS. The Au nano-cluster size and density are determined for four different amounts of Au deposition. It is shown that this nondestructive method can give all mentioned information on such a metalized polymer without the need for any other complimentary and time consuming technique such as AFM, TEM and the destructive technique XTEM. Thus this method is suitable to monitor and control the degree of intermixing of metal nano-clusters and polymers which is of high technological interest.

Keywords: XPS peak shape analysis; Gold nano-clusters; Polystyrene

1. Introduction

Metallization of polymers is of considerable technological importance and is also very interesting from a fundamental point of view. Metalized polymers are used extensively in applications such as food packing, on- chip interconnection, reflectors for car lights, optical data storage (compact discs), electrically shielded computer cases, decorative coatings, optical ultra thin color filters and substrates for biomolecules [1]. In general, the properties of metal/polymer interfaces are determined by the interaction between the metal and the polymer and by the morphology of the interface. The cohesive energy of metals is typically two orders of magnitude higher than the cohesive energy of polymers. Furthermore, the interaction between moderately reactive metals and polymers is generally very weak in comparison to the strong metal–metal binding forces. Therefore, noble metals and other metals of low reactivity do not wet untreated polymer surfaces but form three-dimensional spherical clusters, i.e. they exhibit a Volmer–Weber growth mode [2,3].

The change in Gibbs free energy is the driving force for embedding of metal-clusters in polymers. The Gibbs free energy of a metal particle inside the polymer is lower than that of the particle at the surface. This is related to the high cohesive energy of metals, which gives rise to a correspondingly high surface Gibbs free energy of metal particles. The surface Gibbs free energy can be reduced by embedding if the surface tension γ_M of the metal particles exceeds the sum of the interfacial tension γ_{MP} and the polymer surface tension γ_P [4,5]:

$$\gamma_M > \gamma_{MP} + \gamma_P \quad (1)$$

As mentioned above, the cohesive energy of polymers is much lower than that of metals, therefore γ_P is very small in comparison to γ_M. The embedding of nanometer size

* Corresponding author. Present address: Department of Physics and Chemistry, University of Southern Denmark, DK-5230 Odense M, Denmark. Tel.: +45 504 25831; fax: +45 661 58760.
E-mail address: hajati@fysik.sdu.dk (S. Hajati).

0039-6028/$ - see front matter © 2007 Elsevier B.V. All rights reserved.
doi:10.1016/j.susc.2007.06.001

clusters require long-range chain mobility, which proceeds in experimentally accessible time scales above the glass transition temperature (T_g). Therefore, the embedding process responds to changes in temperature and thereby in chain mobility in a near surface region.

The microstructure and hence the mechanical and dielectric properties of the thin-film may be affected strongly by the cluster size, density and degree of intermixing with nano-clusters [2,6–9]. The cluster density depends on the deposition parameters as well as on the metal–polymer interaction and is in the range 10^{10}–10^{16} cm^{-2} [10]. Therefore, it is of high importance to be able to characterize metal nano-clusters as well as to understand and to control diffusion of metal-clusters in polymers.

Different techniques have been used to study the metal nano-clusters on polymers. For instance, the embedding was analyzed by traditional XPS based on peak intensity [11–13], by small-angle X-ray scattering [14], XTEM [2] and Rutherford backscattering (RBS) [15]. The phenomenon of metal clustering on polymers has been studied by TEM [16] and combined TEM/AFM [17,18]. Recently, Zaporojtchenko et al. showed that information on the size of the clusters not larger than 5 nm can be obtained by measuring the XPS peak intensity ratio for two different transitions from the same metal [19].

In this work, we use XPS peak shape analysis (see theory outlined in Section 2) to study how gold nano-clusters grow, diffuse and distribute in polystyrene as a function of both cluster size and the temperature in the range from below to above the glass transition temperature of the polymer. The size and density of Au nano-clusters are determined for four different amounts of the gold deposition. It is shown that this method can give all mentioned information on such a metalized polymer without the need for any other complimentary and time consuming technique such as AFM, TEM and XTEM.

2. Theory

We use the XPS peak shape analysis method developed by Tougaard et al. [20–29] which relies on the following physical phenomenon. After the photo-excitation process, some of the electrons are transported to the surface and enter the spectrometer. The XPS peak shape and intensity vary dramatically with surface morphology. The reason is that as the electrons move on their way out of the solid, they lose energy. The longer path length they travel, the larger is the fraction of the electrons that have lost energy. For electrons that travel only a short distance, the chance that they lose energy is small and the change in energy distribution is small. For electrons that travel a larger distance, a larger fraction will have lost energy and the intensity at the peak energy is diminished. These electrons are found at lower energies in the spectrum and the distortion of the energy spectrum is substantial. Since the mean distance between inelastic scattering events for 200–1500 eV electrons (which is typical for XPS) is ~0.5–2 nm, the XPS peak shape varies significantly with the distribution, $f(x)$, of atoms on the nanometer depth scale.

A measured XPS spectrum $J(E)$ is a function of the intrinsic distribution, $F(E)$, of primary emitted photo electrons per angstrom, the differential inelastic scattering cross-section, $K(T)$, and the composition depth profile, $f(x)$ [20]. For a correct quantitative analysis, the intrinsic $F(E)$ therefore has to be restored from $J(E)$ by removal of extrinsic contributions under the assumption of the correct $f(x)$ and $K(T)$. Alternatively $f(x)$ can be evaluated from $J(E)$, if $F(E)$ and $K(T)$ are known. When the extrinsic contributions are correctly removed from $J(E)$, $F(E) \approx 0$ in a wide energy interval 50–150 eV on the low energy side of the peak. In situations where the effects of the chemical environment do not significantly affect the intrinsic shape of $F(E)$, the restoration process must give $F(E)$ spectra similar in both intensity and shape in order to be correct.

The general solution for the extraction of $F(E)$ from $J(E)$ were described rigorously as follows [21,22]

$$F(E) = \frac{1}{P_1}\left\{J(E) - \int \mathrm{d}E' J(E) \int_{-\infty}^{+\infty} \mathrm{d}s \exp(\mathrm{i}2\pi s[E' - E]) \times \left[1 - \frac{P_1}{P(s)}\right]\right\} \tag{2}$$

where

$$P_1 = \int_0^\infty \mathrm{d}x f(x) \exp\left(\frac{-x}{\lambda \cos\theta}\right) \tag{3a}$$

and

$$P(s) = \int_0^\infty \mathrm{d}x f(x) \times \exp\left(\frac{-x}{\lambda\cos\theta}\left[1 - \int_0^\infty \mathrm{d}T \lambda K(T) \exp(-\mathrm{i}sT)\right]\right) \tag{3b}$$

and analytical expressions were found for different types of in-depth distributions [21–28]. In the above equations, θ is the angle of detection with respect to the surface normal and λ the inelastic mean free path (IMFP).

For $K(T)$, the following expression (called two-parameter universal cross-section):

$$\lambda K(T) = \frac{BT}{(C + T^2)^2} \tag{4}$$

with $C = 1643$ eV^2 and $B \approx 3000$ eV^2 is a valid approximation for many transition metals as well as for their alloys and oxides [29]. For solids such as Al, Si, SiO_2, and polymers that have a narrower cross-section, it is a better approximation to use

$$\lambda K(T) = \frac{BT}{(C - T^2)^2 + DT^2} \tag{5}$$

where C and D are constants characteristic of the solid [29].

In this work, we will characterize gold nano-clusters before annealing of the samples (at room temperature, RT) applying island growth (Volmer–Weber) mechanism with

$$f(x) = \begin{cases} cf_1, & \text{for } 0 < x < h \\ 0, & \text{otherwise} \end{cases} \quad (6a)$$

where h is the height of the island, f_1 is the fractional surface coverage ($0 \leqslant f_1 \leqslant 1$) with atoms for which the spectrum was acquired and c is the concentration of the pure element. To study the annealing of the samples from RT to 220 °C we will apply buried layer morphology with

$$f(x) = \begin{cases} c', & \text{for } d_0 < x < d_0 + \Delta d \\ 0, & \text{otherwise} \end{cases} \quad (6b)$$

where d_0 is the depth under which the material is buried over the depth interval Δd and c' is concentration of the element over the depth Δd. For details, see Ref. [22].

3. Experimental

Monodisperse polystyrene (PS) with $M_w = 212000$ g/mol and $M_w/M_n < 1.1$ used in the experiments was obtained from Aldrich Chemical Company as powder where M_w and M_n are weight average molecular weight and number average molecular weight of the polymer, respectively. The polystyrene films (thickness of approximately 200 nm) were prepared by dissolving the polymer powder in toluene (27 g/l) and spin coating it on a silicon wafer with its native oxide layer. PS samples were annealed under vacuum conditions for 40 min at a temperature of 130 °C and then slowly cooled down to room temperature (RT) with constant cooling rate of 1 °C/min.

Four samples with different gold depositions of 2, 8, 14 and 24 Å nominal thickness were made. To make each sample, the substrate temperature was constantly kept at room temperature during Au deposition. Gold (99.99% pure, Good Fellow Industries) was evaporated from a heated Mo crucible mounted in the preparation chamber of the XPS spectrometer (Omicron Full Lab). The deposition rate and the nominal thickness rate were monitored by a quartz crystal microbalance (QCM), which was calibrated gravimetrically.

Samples with 2 Å and 8 Å nominal thickness were heated with a ramp 1 K/min in the XPS-chamber and data acquisition was made after achieving some definite temperature T (the sample was kept at this T for ~5 min without cooling) using monochromatic Al Kα radiation.

4. Analysis and results

To analyze the XPS Au4f spectra obtained from gold nano-clusters on polystyrene, we used the QUASES-Tougaard software package [28] which was set up based on the theory in Section 2 and references therein. The Au 4f photoelectrons were excited by Al Kα radiation and we used $\lambda = 15.78$ Å for gold (calculated with the QUASES-TPP-2M calculator which can be freely downloaded from www.quases.com; this calculator uses the TPP-2M formula due to Tanuma et al. [30]). The Au 4f photoelectrons were detected normal to the surface ($\theta = 0$).

We have studied two issues: Au nano-cluster growth mechanism at RT and annealing induced redistribution of the Au nano-clusters.

Fig. 1 shows the Au 4f spectra at RT after deposition of varying amounts of Au. We analyze these spectra based on the XPS peak shape and thereby determine the nano-cluster formation, cluster size and the number of clusters per unit area (n) on the polystyrene surface. It is expected that they form spheres, due to very high cohesive energy of Au and very low reactivity between Au and PS. We now make a model taking this into account in the analysis by considering the corresponding $f(x)$. To this end, we divide spheres (with diameter $2R$ and surface coverage f_1) into nine coaxial cylindrical shells with the same surface coverage and different h (see Fig. 2). In this model, the following rules apply for the parameters characteristic of the cylindrical islands:

$$h_i = 2R \times \sqrt{1 - \left(\frac{\sqrt{i} + \sqrt{i-1}}{6}\right)^2}, \quad i = 1, 2, \ldots, 9 \quad (7)$$

$$f_{1i} = f_1/9, \quad i = 1, 2, \ldots, 9 \quad (8)$$

$$\sum_{i=1}^{9} h_i f_{1i} = T_{\text{eff}} \quad (9)$$

where i, h_i and f_{1i} are the index, the height and the surface coverage of each island, respectively, and T_{eff} is the effective thickness of Au deposition.

Now, it is possible to determine the cluster size ($2R$) and coverage (f_1) of the Au clusters for each deposition by using a gold reference $F(E)$ spectrum (see Ref. [22]). Usually one would obtain that from analysis of the spectrum taken from a pure Au sample. However, since we know T_{eff} of the Au overlayer for each deposition from the values measured by QCM, we can use the sample with the highest effective thickness $T_{\text{eff}} = 24$ Å as a reference. We adjust $2R$ (or h_i) until the corrected spectrum has $F(E) \approx 0$ in a wide kinetic

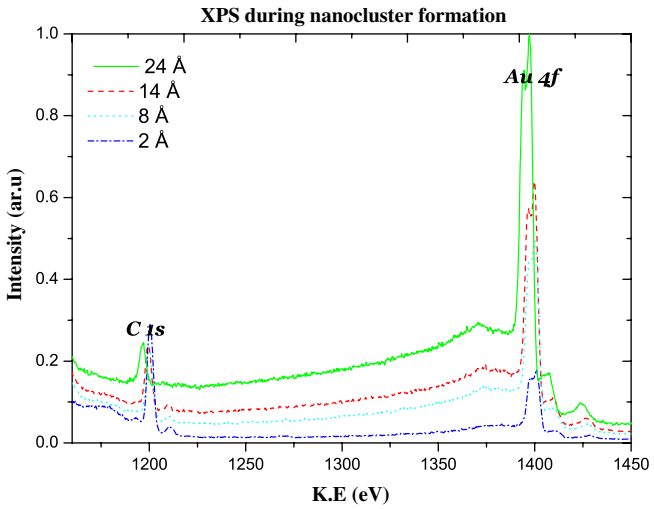

Fig. 1. The Au 4f spectra taken from samples with effective gold thickness $T_{\text{eff}} = 2$ Å, 8 Å, 14 Å and 24 Å at RT.

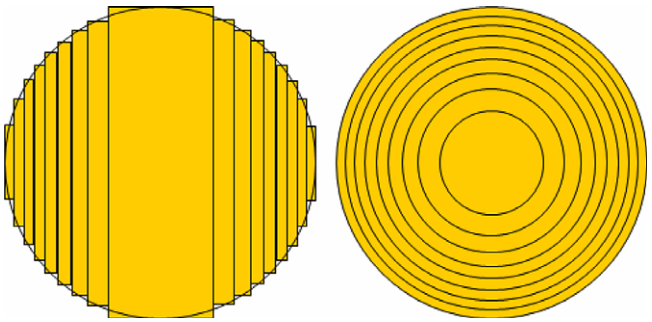

Fig. 2. Dividing spheres (with diameter $2R$ and surface coverage f_1) into nine coaxial cylindrical shells with the same surface coverage and different h for the box Island model in QUASES-Tougaard being applicable to spherical nano-clusters, side view (left), top view (right).

energy interval 50–150 eV below the peak energy (see Fig. 3), and then by applying Eqs. (8) and (9), the coverage f_1 is obtained. To analyze the spectra for other samples, we adjust $2R$ (or h_i) to get $F(E)$ with the same shape as the $F(E)$ obtained by using the reference (see Fig. 3), and then we adjust f_{1i} to get the same peak area as for the reference $F(E)$ (see Fig. 4). Note the very good agreement between the obtained $F(E)$ for all four different depositions.

Fig. 5 shows the obtained cluster size ($2R$) for different Au depositions. Fig. 6 shows T_{eff} obtained for each deposition from Eq. (9), plotted against the values measured by QCM. Note the very good agreement with deviations less than 5% on an absolute scale.

To calculate n (the number of clusters per cm^2), we can use the following formula:

$$n = \frac{f_1}{\pi R^2} \times 10^{16} \tag{10}$$

where πR^2 is the projected area of a given spherical cluster and R is in Å. The obtained n for effective thicknesses 2, 8, 14 and 24 Å are shown in Fig. 7. For comparison, Fig. 8 shows a TEM image of a sample with 3 Å effective thickness of deposited gold. Analysis of this image gives an average cluster size of 30 ± 2Å and a cluster density

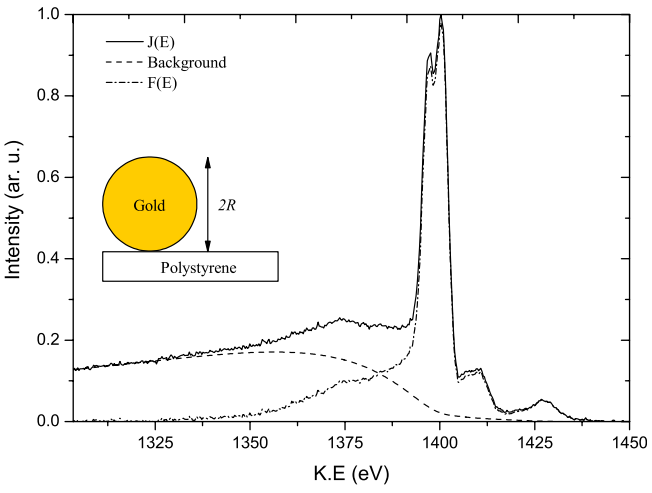

Fig. 3. Analyzed Au 4f spectrum for $T_{\text{eff}} = 24$ Å at RT.

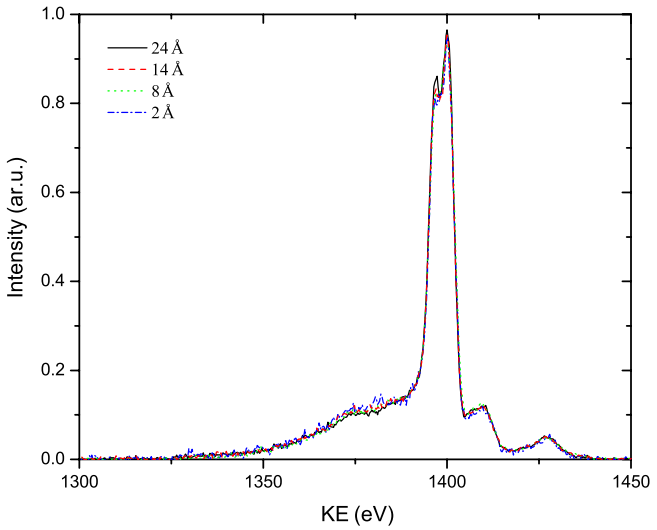

Fig. 4. The obtained $F(E)$ after analyzing Au 4f signals taken from the samples with effective gold thickness $T_{\text{eff}} = 2$ Å, 8 Å, 14 Å and 24 Å at RT.

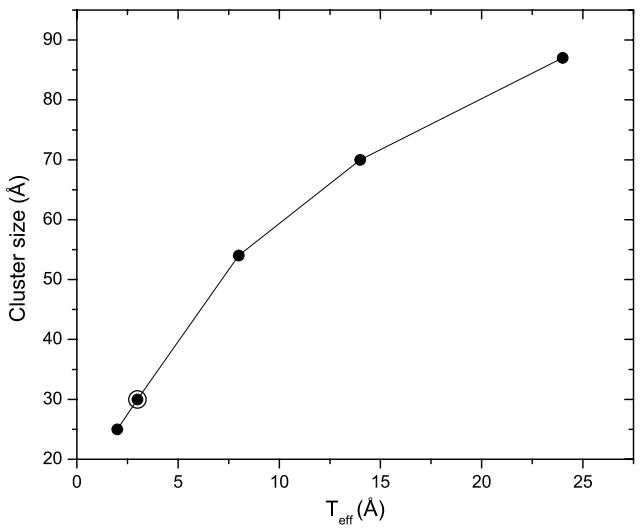

Fig. 5. Cluster size ($2R$) determined by QUASES-Tougaard analysis for different Au depositions at RT on PS. The value for 3 Å deposition (centered circle) was determined from the TEM image in Fig. 8.

2.0×10^{12} cm^{-2}. The values are also shown in Figs. 5 and 7 (centered circle), respectively, and are seen to be in good agreement with the values determined by the XPS peak shape analysis.

It is of interest to study to what extent island coalescence takes place as the Au deposition increases. From Fig. 7, we see that the cluster density determined by XPS peak shape analysis, clearly decreases for increasing Au deposition. From this, we can conclude that coalescence happens.

We measured a series of XPS spectra during annealing of the samples from RT, i.e. below the glass transition temperature ($T_g \approx 100$ °C) of PS to 220 °C which is well above T_g and below its melting point (~240 °C). These series of data were acquired from samples with 2 Å and 8 Å gold deposition. For embedded nano-clusters, the QUASES-

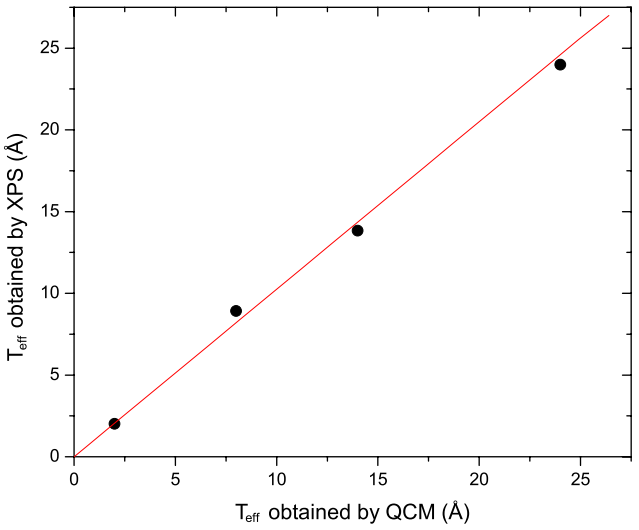

Fig. 6. Obtained T_{eff} by QUASES-Tougaard analysis, for each Au deposition at RT, compared to the values measured by QCM. The line is fitted to the points.

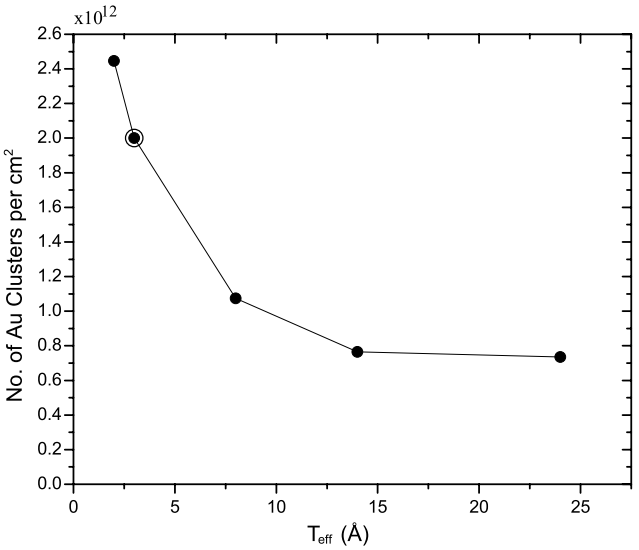

Fig. 7. Number of Au clusters per cm^2 determined by QUASES-Tougaard analysis for different Au depositions at RT. The value for 3 Å deposition (centered circle) was determined from the TEM image in Fig. 8.

Tougaard software cannot use spherical model. Although they are actually spheres, either the spherical (nine box model, Eqs. (7)–(9)) or the one box model (Eqs. (6a) and (6b)) results in $F(E)$ with the same quality as in Fig. 4. This shows that we can use the box model. Therefore, for this part of analysis, we use box model which gives smaller height. For XPS peak shape analysis of the spectra taken at each step of annealing, we adjust d_0, Δd and c', Eq. (6b), to obtain $F(E)$ with the same shape and intensity as the reference spectrum. The fact that the height of spheres with a given volume are larger than that of the boxes with the same volume as well as the same cross-section area by a factor of 1.5 and also the fact that they are actually spheres, require to correct the obtained values by that factor. The

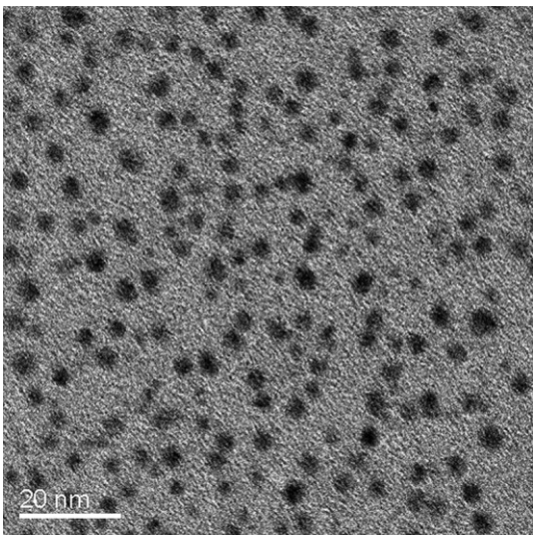

Fig. 8. TEM image of a sample with 3 Å effective thickness of deposited gold at RT.

corrected results, Δd_1 and Δd_2, are shown in Fig. 9. As a check on the consistency of the analysis, we can calculate the determined amount of Au atoms by multiplying c' by the obtained Δd for each step of annealing of the samples (see Fig. 10). It is seen to be constant to within less than 15% at all annealing temperatures. In the calculations, we used the universal cross-section, Eq. (4). The actual cross-section is expected to be a weighted average of the universal and the polymer cross-section depending on the degree of intermixing of metal-clusters and polymers. Likewise, the

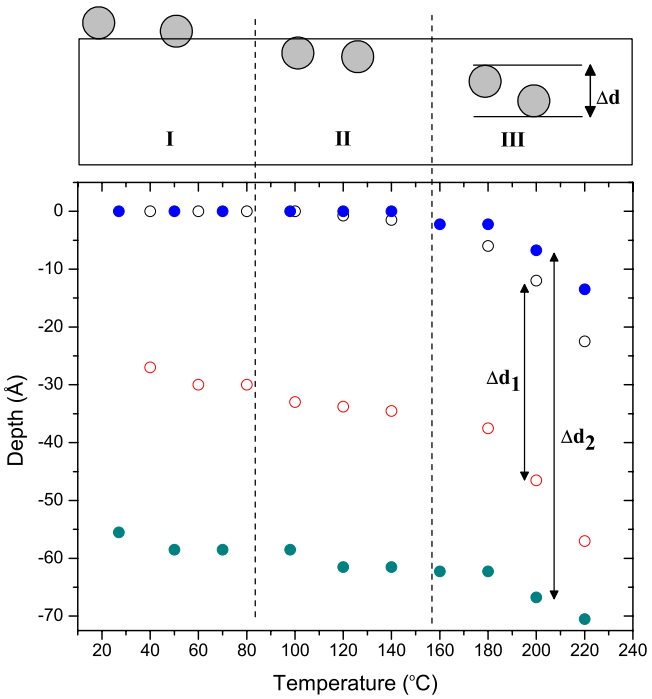

Fig. 9. Depth profile for 2 Å (open circle) and 8 Å (solid circle) Au deposition as a function of temperature. Δd_1 and Δd_2 are the depth interval over which the nano-clusters are distributed corresponding to 2 Å and 8 Å Au deposition, respectively.

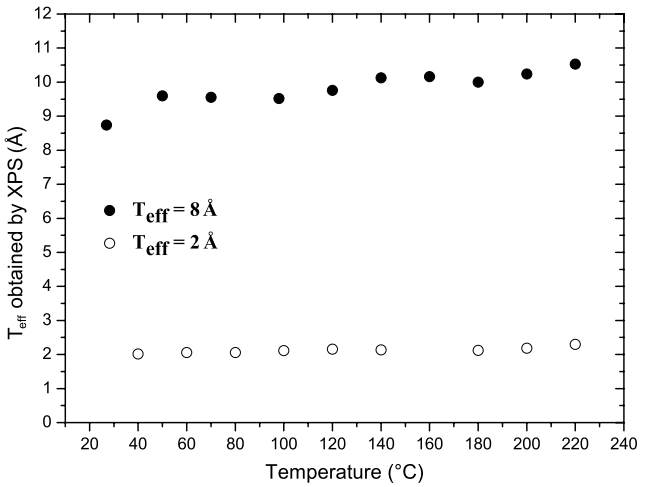

Fig. 10. T_{eff} for 2 Å (open circle) and 8 Å (solid circle) Au deposition measured by XPS peak shape analysis during the annealing of the samples.

effective IMFP is expected to change gradually as the gold nano-clusters are embedded. These effects are likely to be the reason for the small gradually increase in T_{eff} observed in Fig. 10.

5. Discussion

As demonstrated in this paper, the XPS peak shape analysis is an easy method to study structure and depth distribution of nano-clusters because only a single XPS spectrum is required. It is therefore easy to study the redistribution of nano-clusters during growth as well as gradual annealing. And it is also a nondestructive method to investigate the degree of intermixing of metal-clusters and polymers. In comparison, to do this study by XTEM [2] it is required to cut the sample which is time consuming and it is destructive and the continuous evolution with annealing cannot be followed for the exact same sample.

Compared to AFM and TEM, the XPS peak shape analysis method is very easy and fast because all information on the cluster size as well as on the cluster distribution is obtained from analysis of a single XPS spectrum. Furthermore, clusters at high density cannot be resolved by contact mode AFM when the tip size is larger than the lateral spacing between neighboring clusters [31]. XPS peak shape analysis does not have this limitation. Moreover, the size of the metallic clusters can be measured directly by TEM but due to contrast and focusing limitations, it is difficult to determine accurate sizes for small clusters with radii in the range 0.5–2 nm [19], which however is the most interesting size range for the determination of the initial stages of film growth. Also, the preparation of transparent polymer samples for TEM is difficult.

6. Conclusion

We conclude that XPS peak shape analysis, which is a *nondestructive* method, is an efficient method to study quantitatively how metal nano-clusters grow, diffuse and distribute on and in a polymer as a function of cluster size and the temperature in the range from room temperature to considerably above the glass transition temperature of the polymer.

The important point is that this method can give all mentioned information on such a metalized polymer without the need for any other complimentary and time consuming technique such as AFM, TEM and XTEM. Therefore, it can stand-alone and is also suitable to monitor and control the degree of intermixing of metal-clusters and polymers which is of high technological importance.

Consequently, XPS peak shape analysis is fast, simple to handle and powerful for quality control in mass production of metal–polymer nano-materials.

Acknowledgments

We thank Dr. J. Zekonite for his help in the preparation of the sample for TEM measurement. The support by the Iranian Ministry of Science, Research and Technology (Project No. 42/5/58107-12/8/83) is acknowledged.

References

[1] K.L. Mittal (Ed.), Metalized Plastics: Fundamentals and Applications, Marcel Dekker, New York, 1998.
[2] F.K. LeGoues, B.D. Silverman, P.S. Ho, J. Vac. Sci. Technol. A 6 (1988) 2200.
[3] F. Faupel, T. Strunskus, M. Kiene, A. Thran, C. von Bechtolsheim, V. Zaporojtchenko, Mater. Res. Soc. Symp. Proc. 511 (1998) 15.
[4] G.J. Kovacs, P.S. Vincett, J. Colloid Interface Sci. 90 (1982) 335.
[5] G.J. Kovacs, P.S. Vincett, C. Tremblay, A.L. Pundsack, Thin Solid Films 101 (1983) 21.
[6] P.S. Ho, R. Haight, R.C. White, B.D. Silverman, F. Faupel, in: L.H. Lee (Ed.), Fundamentals of Adhesion, Plenum, New York, 1991, p. 383.
[7] R.M. Tromp, F.K. LeGoues, P.S. Ho, J. Vac. Sci. Technol. A 3 (1985) 782.
[8] S.P. Kowalczyk, Y.H. Kim, G.F. Walker, J. Kim, Appl. Phys. Lett. 52 (1988) 375.
[9] F. Faupel, in: J.J. Pireaux, P. Bertrand, J.L. Brédas (Eds.), Polymer–Solid Interfaces, IOP Publishing, 1992, p. 171.
[10] V. Zaporojtchenko, J. Zekonyte, A. Biswas, F. Faupel, Surf. Sci. 532–535 (2003) 300.
[11] V. Zaporojtchenko, T. Strunskus, J. Erichsen, F. Faupel, Macromolecules 34 (2000) 1125.
[12] J. Erichsen, K. Günther-Schade, K. Dolgner, T. Strunskus, V. Zaporojtchenko, F. Faupel, Mater. Res. Soc. Symp. Proc. 710 (2002) DD14.5.
[13] J. Erichsen, J. Kanzow, U. Schürmann, K. Dolgner, K. Günther-Schade, T. Strunskus, V. Zaporojtchenko, F. Faupel, Macromolecules 37 (2004) 1831.
[14] R. Weber, K.-M. Zimmermann, M. Tolan, J. Stettner, W. Press, O.H. Seeck, J. Erichsen, V. Zaporojtchenko, T. Strunskus, F. Faupel, Phys. Rev. E 64 (2001) 61508.
[15] N. Marin, Y. Serruys, P. Calmon, Nucl. Instr. Meth. Phys. Res. B 108 (1996) 79.
[16] S. Faghihi, T. Hoffmann, J. Petermann, J. Martinez-Salazar, Macromolecules 25 (1992) 2509.
[17] K.D. Jandt, M. Buhk, J. Petermann, L.M. Eng, H. Fuchs, Mater. Res. Soc. Symp. Proc. 280 (1993) 245.
[18] K.D. Jandt, T.J. McMaster, M.J. Miles, J. Petermann, Macromolecules 26 (1993) 6552.

[19] V. Zaporojtchenko, K. Behnke, T. Strunskus, F. Faupel, Surf. Interface Anal. 30 (2000) 439.
[20] S. Tougaard, P. Sigmund, Phys. Rev. B 25 (1982) 4452.
[21] S. Tougaard, Surf. Interface Anal. 11 (1988) 453.
[22] S. Tougaard, H.S. Hansen, Surf. Interface Anal. 14 (1989) 730.
[23] S. Tougaard, J. Vac. Sci. Technol. A 8 (1990) 2197.
[24] S. Tougaard, J. Electron. Spectrosc. 52 (1990) 243.
[25] S. Tougaard, J. Vac. Sci. Technol. A 14 (1996) 1415.
[26] S. Tougaard, Appl. Surf. Sci. 100/101 (1996) 1.
[27] S. Tougaard, Surf. Interface Anal. 26 (1998) 249.
[28] S. Tougaard, QUASES-Tougaard: Software Package for Quantitative Analysis of Surface by Electron Spectroscopy, Version 5.1, 2005. See http://www.quases.com.
[29] S. Tougaard, Surf. Interface Anal. 25 (1997) 137.
[30] S. Tanuma, C.J. Powell, D.R. Penn, Surf. Interface Anal. 21 (1993) 165.
[31] J. Knall, J.B. Pethica, Surf. Sci. 265 (1992) 156.